

# APOBEC3B interaction with PRC2 modulates microenvironment to promote HCC progression

Duowei Wang,<sup>1</sup> Xianjing Li,<sup>1</sup> Jian Li,<sup>1</sup> Yuan Lu,<sup>1</sup> Sen Zhao,<sup>1</sup> Xinying Tang,<sup>1</sup> Xin Chen,<sup>1</sup> Jiaying Li,<sup>1</sup> Yan Zheng,<sup>1</sup> Shuran Li,<sup>1</sup> Rui Sun,<sup>1</sup> Ming Yan,<sup>1</sup> Decai Yu,<sup>2</sup> Guangwen Cao,<sup>3</sup> Yong Yang<sup>1</sup>

► Additional material is published online only. To view please visit the journal online (<http://dx.doi.org/10.1136/gutjnl-2018-317601>).

<sup>1</sup>Center for New Drug Safety Evaluation and Research, State Key Laboratory of Natural Medicines, China Pharmaceutical University, Nanjing, China

<sup>2</sup>Department of General Surgery, The Affiliated Drum Tower Hospital, Medical School of Nanjing University, Nanjing, China

<sup>3</sup>Department of Epidemiology, Second Military Medical University, Shanghai, China

## Correspondence to

Professor Yong Yang, Center for New Drug Safety Evaluation and Research, State Key Laboratory of Natural Medicines, China Pharmaceutical University, Nanjing 210017, China; yy@cpu.edu.cn

DW, XL, JL and YL contributed equally.

Received 14 September 2018

Revised 22 April 2019

Accepted 12 May 2019

Published Online First

1 June 2019

## ABSTRACT

**Objective** APOBEC3B (A3B), a cytidine deaminase acting as a contributor to the APOBEC mutation pattern in many kinds of tumours, is upregulated in patients with hepatocellular carcinoma (HCC). However, APOBEC mutation patterns are absent in HCC. The mechanism of how A3B affects HCC progression remains elusive.

**Design** A3B promoter luciferase reporter and other techniques were applied to elucidate mechanisms of A3B upregulation in HCC. A3B overexpression and knockdown cell models, immunocompetent and immune-deficient mouse HCC model were conducted to investigate the influence of A3B on HCC progression. RNAseq, flow cytometry and other techniques were conducted to analyse how A3B modulated the cytokine to enhance the recruitment of myeloid-derived suppressor cells (MDSCs) and tumour-associated macrophages (TAMs).

**Results** A3B upregulation through non-classical nuclear factor- $\kappa$ B (NF- $\kappa$ B) signalling promotes HCC growth in immunocompetent mice, associated with an increase of MDSCs, TAMs and programmed cell death1 (PD1) expressed CD8 $^{+}$  T cells. A CCR2 antagonist suppressed TAMs and MDSCs infiltration and delayed tumour growth in A3B and A3B $E68Q/E255Q$  expressing mouse tumours. Mechanistically, A3B upregulation in HCC depresses global H3K27me3 abundance via interaction with polycomb repressor complex 2 (PRC2) and reduces an occupancy of H3K27me3 on promoters of the chemokine CCL2 to recruit massive TAMs and MDSCs.

**Conclusion** Our observations uncover a deaminase-independent role of the A3B in modulating the HCC microenvironment and demonstrate a proof for the concept of targeting A3B in HCC immunotherapy.

## Significance of this study

### What is already known on this subject?

- APOBEC3B (A3B) and APOBEC3A (A3A) induced APOBEC mutagenesis pattern is absent in hepatocellular carcinoma (HCC).
- A3B is upregulated in patients with HCC and chronic HBV infection.
- MDSCs and TAMs are abundant in HCC microenvironment and are often associated with poor prognosis.
- Chemokine expression is regulated by cancer-intrinsic genetic and epigenetic mechanisms such as the DNA methylation, the H3K27me3 and polycomb repressor complex 2 (PRC2).

### What are the new findings?

- The non-canonical NF- $\kappa$ B signalling pathway stimulates A3B expression and that RelB directly binds to the GGGGAAAC sequence at the A3B gene promoter to activate its transcription.
- The hepatoma-intrinsic A3B mediates MDSCs and TAMs accumulation by CCL2 to promote HCC progression.
- Harmonious overexpression of A3B and TAM/MDSC markers correlates with poor prognosis of patients with HCC.
- A3B interaction with PRC2, which is independent of cytosine deaminase pathways, depresses global H3K27me3 abundance and reduces an occupancy of H3K27me3 on promoters of the chemokine CCL2 to recruit massive MDSCs and TAMs.

### How might it impact on clinical practice in the foreseeable future?

- These findings elucidate a novel therapeutic target in HCC that expand the immunosuppressive microenvironment.
- Developing novel compounds to interrupt the interaction of A3B and PRC2 complexes might be a new strategy for HCC immunotherapy.

## INTRODUCTION

The apolipoprotein B mRNA editing enzyme catalytic polypeptide-like 3B (APOBEC3B (A3B)) is 1 of 11 in the AID/APOBEC family.<sup>1</sup> It is a cytosine deaminase that catalyses conversion of cytosine to uracil and leads to the mutation of the substrate DNA sequence. Multiple studies analysing the DNA mutations caused by A3B and A3A uncovered an APOBEC cytidine deaminase mutagenesis pattern widespread in human cancers including bladder, breast, cervix and thyroid cancer and so on.<sup>2–3</sup> However, APOBEC mutation pattern is absent in HCC,<sup>4–5</sup> although A3B is upregulated in patients with chronic HBV infection or HCC.<sup>6–7</sup> In

a recent study, it was found that APOBEC mutation pattern occurs on the Okazaki fragment during DNA replication.<sup>8</sup> Interestingly, the genome mutation signal for liver cancer occurs during the transcription process.<sup>9</sup> Furthermore, A3B



► <http://dx.doi.org/10.1136/gutjnl-2019-319084>



© Author(s) (or their employer(s)) 2019. No commercial re-use. See rights and permissions. Published by BMJ.

To cite: Wang D, Li X, Li J, et al. Gut 2019;68:1846–1857.

overexpression-induced lymphotxin- $\beta$  receptor activation does not affect genomic DNA.<sup>10</sup> These results showed that the cytosine deaminase activity of A3B is tightly controlled to prevent mutation of genomic DNA. The mechanism of how A3B affects HCC progression remains elusive.

The incidence of HCC is closely related to the background of chronic inflammation that results in a change of number and function of immune cell subpopulations, such as T cells, MDSCs and macrophages.<sup>11</sup> The interaction between immune cells and hepatoma through inflammatory factors results in egress of immature myeloid cells from the bone marrow into the tumour sites. MDSCs and TAMs are abundant in the HCC microenvironment and are often associated with poor prognosis.<sup>12</sup> MDSCs and TAMs suppress CD8 $^{+}$  T cell function by depriving amino acids via arginase-I expression, releasing oxidising molecules and stimulating other immunosuppressive cells. Here, we investigate the mechanism by which A3B promotes the expression of chemokine, leading to an increase in MDSCs and TAMs, resulting in an immunosuppressive microenvironment and tumour progression.

## METHODS

The C57BL/6J mice and Balb/C Nude mice were purchased from Shanghai SLAC Laboratory Animal Co, Ltd. All animal experiments were conducted with the approval of the Center for New Drug Evaluation and Research, China Pharmaceutical University (Nanjing, China) and in accordance with the National Institutes of Health Guide for the Care and Use of Laboratory Animals. Please see details in the online supplementary materials and methods.

## RESULTS

### A3B is highly expressed in HCC and correlates with poor prognosis

To investigate the contribution of the AID/APOBEC family to HCC, we mined TCGA transcriptome datasets to compare levels of each gene between HCC tissues and normal tissues at the GAPIA website. Only A3B mRNA was upregulated significantly in HCC tissues, whereas A3A mRNA trended towards downregulation (figure 1A and online supplementary figure

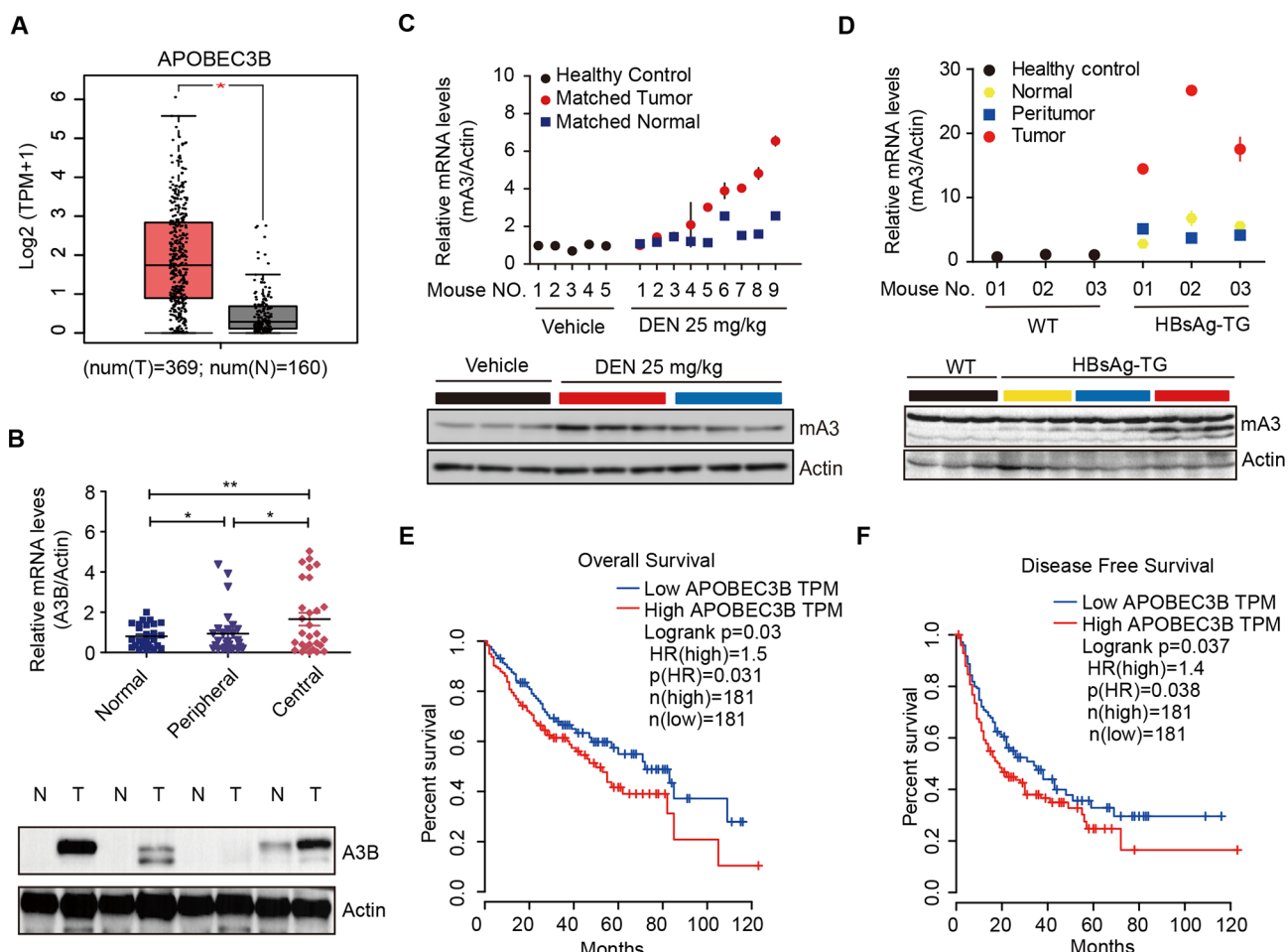


**Figure 1** A3B was highly expressed in liver cancer and correlates with poor prognosis in HCC patients. (A) A3B expression levels in HCC ( $n=369$ ) and non-tumour tissues ( $n=160$ ) in GEPIA database. The differential analysis here is based on the selected datasets with TCGA tumours versus TCGA normal+GTEx normal. Data are presented as the mean $\pm$ SEM. \* $p<0.01$  (one-way ANOVA). (B) RT-qPCR and immunoblot assays of A3B mRNA and protein levels in human normal, peripheral and central liver cancer tissues. \* $P<0.05$ , \*\* $p<0.01$  (Student's t-test). (C and D) RT-qPCR and immunoblot assays of mA3 mRNA and protein levels in the DEN-induced HCC mouse model ( $n=5$  mice in vehicle group and  $n=9$  in DEN group) (C) and HBsAg transgenic mice ( $n=3$  mice per group) (D) in normal, peritumor and tumour tissues of HBsAg transgenic mice. (E and F) Kaplan-Meier overall survival (E) and disease-free survival (F) curves of patients with HCC with high ( $n=181$ ) and low ( $n=181$ ) expressions (stratified by median) of A3B mRNAs in the GEPIA database using TCGA data (log-rank test). A3B, APOBEC3B; ANOVA, analysis of variance; DEN, N-nitrosodiethylamine; HBsAg, hepatitis B surface antigen; HCC, hepatocellular carcinoma; TPM, transcripts per kilobase million; WT, wild type.

1A). Similar findings were also observed in an independent GEO dataset of human HCC (GSE45436) (online supplementary figure 1B). To clarify this point further, we quantified mRNA levels for each of the APOBEC3 family members in HCC tissues and adjacent normal liver tissues. The results showed that only A3B was higher in HCC tissues (figure 1B and supplementary figure 1C). Reverse transcription quantitative PCR (RT-qPCR) did not, however, pick up the expression of A3A in HCC tissues and adjacent normal liver tissues (online supplementary figure 1C). The protein level of A3B in HCC tissues (T) was also higher than non-tumour tissues (N) (figure 1B). We further evaluated expression of murine APOBEC3 (mA3) in N-nitrosodiethylamine (DEN)-induced and hepatitis B surface antigen (HBsAg) transgenic mouse HCC models. The results showed that mA3 was increased in tumour tissues as compared with adjacent normal liver tissues in both mouse HCC models (figure 1C,D). Kaplan-Meier analysis of the TCGA dataset revealed that only high levels of A3B mRNA were associated with poor overall survival and disease-free survival of patients with HCC (online supplementary figure 2, figure 1E,F). Together, these data indicated that only A3B was highly expressed in HCC as compared with other AID/APOBEC family members and was associated with poor clinical outcomes in patients with HCC.

### A3B is a novel direct non-canonical NF- $\kappa$ B target gene in HCC cells

Previous findings had shed light on lymphotoxin, which played a fundamental role for initiation and progression of HCC.<sup>13</sup> LT $\alpha_1\beta_2$  could stimulate the NF- $\kappa$ B signal pathway, in which both RelA and RelB were activated. Furthermore, we found several  $\kappa$ B sites in the promoter of A3B using JASPAR database. We next tested if lymphotoxin could upregulate A3B expression in HCC cells. For this purpose, HepG2 cells were exposed to different doses of LT $\alpha_1\beta_2$  for 24 hours. RT-qPCR assays showed that A3B mRNA is significantly upregulated by LT $\alpha_1\beta_2$ , whereas lipopolysaccharide moderately increased A3B expression (figure 2A). A3B protein levels were also elevated by LT $\alpha_1\beta_2$  in HepG2 cells (figure 2A). We next overexpressed RelA or RelB in HepG2 cells. Only RelB was able to increase A3B expression in HepG2 cells (figure 2B). To determine whether A3B is a direct RelB target gene, ChIP-qPCR assays were applied, and the results showed that occupancy of RelB on the A3B promoter was significantly increased by LT $\alpha_1\beta_2$  in HepG2 cells (figure 2C), whereas occupancy by RelA was not increased (data not show). We next examined the sequence of -1204/+107 of the A3B promoter region to identify  $\kappa$ B sites using the NF- $\kappa$ B PBM dataset. The results showed that the sequence of -116 (GGGGAAAACC) is a high affinity  $\kappa$ B site for the RelB/p52 complex, whereas the -1204/+107 sequence has no high affinity  $\kappa$ B sites for the RelA/p50 complex. We conducted DNA pull-down assays to examine binding of RelA or RelB to the A3B promoter in vitro. We constructed a DNA probe containing -456 to +107, in which it contains multiple sequences similar to the  $\kappa$ B sites, to detect its binding to RelA or RelB in nuclear extracts. Similar findings were obtained that RelB bind to the DNA probe was detected in the HepG2 cell line treated with LT $\alpha_1\beta_2$  (figure 2D). To assess the activity of RelB bind to DNA in -116 promoter region of A3B, we performed DNA pull-down assays using a biotinylated GGGGAAAACC sequence. Immunoblotting of the precipitates confirmed that RelB strongly binds to the DNA sequence which, however, was greatly diminished when a mutant control oligonucleotide was used (figure 2E). Next, we constructed a luciferase reporter plasmid containing

the A3B promoter region from -1204 to +107 (P-Gluc), and two mutant reporter plasmids in -116 (PM1-Gluc) and -68 (PM2-Gluc), a NF- $\kappa$ B site of previous report. Overexpression of RelB significantly enhanced P-Gluc and PM2-Gluc but not PM1-Gluc-driven luciferase in HEK293T cells (figure 2F). Similarly, A3B mRNA was significantly upregulated by LT $\alpha_1\beta_2$  in HCCLM3 and PLC/PRF/5 (figure 2G). In TCGA database, A3B expression in HCC patients moderately correlated with expression of NFBK2 and slightly correlated with RelB, which are the non-canonical NF- $\kappa$ B transcription factors (figure 2H). Taken together, these results indicated that the non-canonical NF- $\kappa$ B signalling pathway stimulates A3B expression and that RelB directly binds to the GGGGAAAACC sequence at the A3B promoter to activate its transcription.

### A3B promotes HCC progression in vivo associated with MDSCs and TAMs accumulation

Here we evaluated the effect of A3B on cell proliferation in a loss and gain of function experiments in vitro. We first analysed the expression of A3B in normal cell line L02 and HCC cell lines. It was shown that the expression of A3B was increased in HCC cell lines compared with that in L02 (online supplementary figure 3). A3B expression failed to induce proliferation in HepG2 in vitro (online supplementary figure 3B,C). Knockdown of A3B similarly failed to suppress proliferation in MHCC97H and MHCC97L cells in vitro (online supplementary figure 3). Furthermore, knockdown of A3B did not alter the growth rate of MHCC97H cells in orthotopic transplantation tumour model in nude mice (online supplementary figure 3H,I). These results suggested that A3B expression in the transformed epithelial compartment is not crucial for the proliferation of HCC in an immunosuppressive microenvironment.

In fact, HCC most commonly develop due to underlying chronic liver inflammation and an altered immune response.<sup>14</sup> Thus, we postulated that hepatoma-intrinsic A3B promoted tumour progression by changing the immune microenvironment. A3B-overexpression Hepa1-6 mouse cell line was generated by the sleeping beauty transposon system (figure 3A).<sup>15</sup> The expression of A3B in Hepa1-6 mouse cell lines similarly failed to induce proliferation in vitro (figure 3B). We next constructed an orthotopic transplantation tumour model in C57BL/6J mice. Expectedly, the liver index and tumour burden of the mice receiving Hepa1-6-A3B cells were significantly higher (figure 3C). We analysed the inflammatory infiltrate in Hepa1-6 orthotopic transplantation tumours. An elevated infiltration of TAMs (figure 3D) and MDSCs were observed in Hepa1-6-A3B tumours (figure 3E). The percentage of CD8<sup>+</sup>PD1<sup>+</sup> T cells significantly increased in Hepa1-6-A3B tumours (figure 3F). Furthermore, CD8<sup>+</sup> PD1<sup>+</sup> T cells in Hepa1-6-A3B tumours exhibited an exhausted phenotype with low expression of granzyme B (figure 3G), perforin (figure 3H) and interferon  $\gamma$  (figure 3I). Moreover, the percentage of spleen MDSCs were significantly increased in the Hepa1-6-A3B model (figure 3J), whereas the percentage of spleen CD8<sup>+</sup> T cells were distinctly decreased in the Hepa1-6-A3B model (figure 3K).

In addition, overexpression of A3B increased the chemoattraction of Hepa1-6 cells to iBMDM in vitro (figure 3L). We analysed mRNA expression in bone marrow-derived macrophages (BMDMs) stimulated in vitro with the conditioned medium. Macrophages with the conditioned medium from Hepa1-6-A3B cells displayed upregulated expression of immunosuppressive molecules, including interleukin (IL)-10 and ARG1. In contrast, immune-activated genes, such as IL-12a were reduced (online

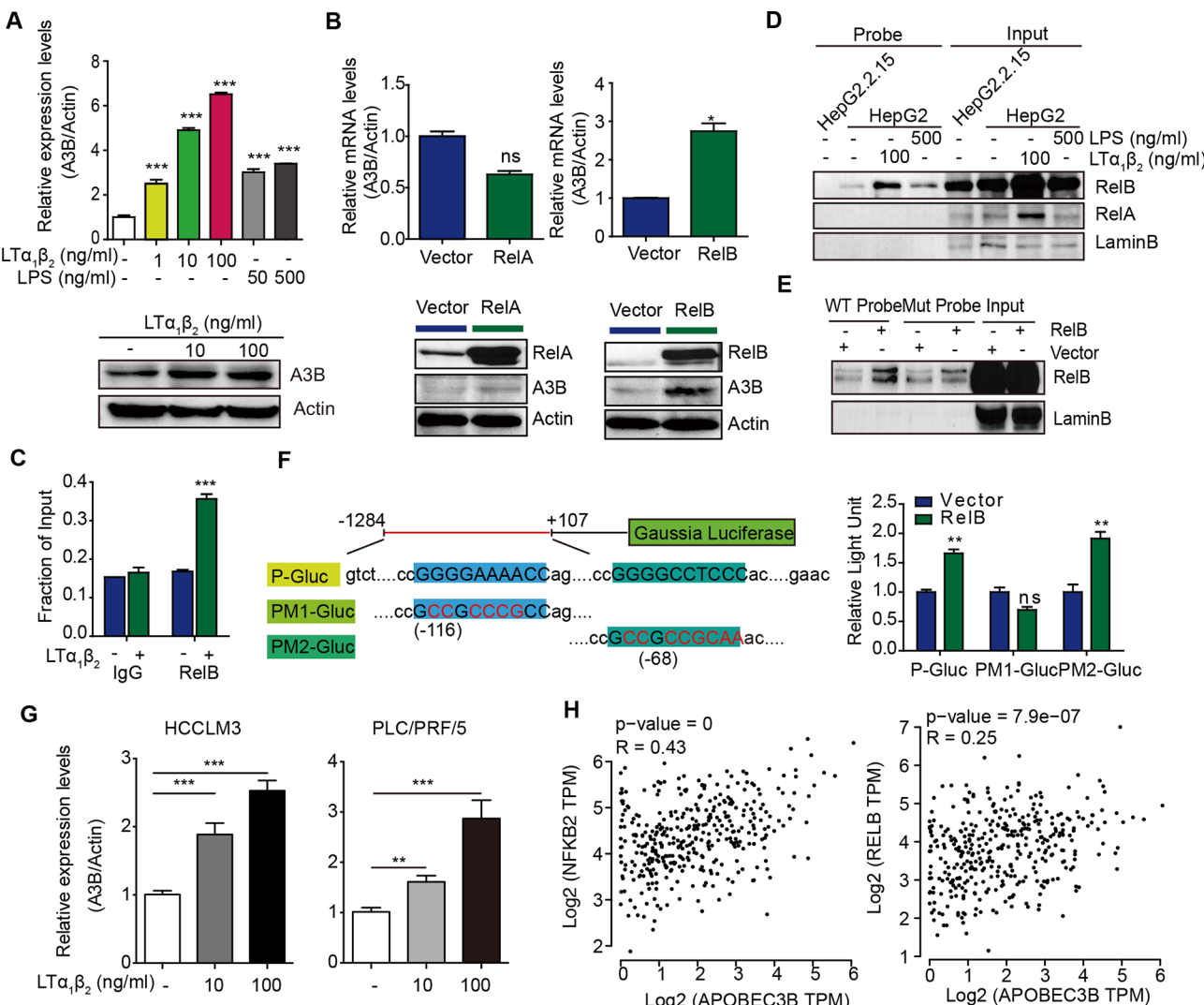


**Figure 2** Lymphotxin upregulates A3B expression through a non-canonical NF- $\kappa$ B pathway. (A) RT-qPCR and immunoblot assays of A3B mRNA and proteins levels in HepG2 cells exposed to LT $\alpha_1\beta_2$  for 24 and 48 hours. (B) RT-qPCR and immunoblot assays of A3B mRNA and protein levels in HepG2 cells transfected with control, RelA plasmid and RelB plasmid for 24 hours. (C) ChIP-qPCR assays in HepG2 cells exposed to LT $\alpha_1\beta_2$  for 12 hours. (D) DNA pull-down assay using a biotinylated DNA probe corresponding to the -456/+107 region of the A3B promoter in HepG2 cells exposed to LT $\alpha_1\beta_2$  for 12 hours. (E) DNA pull-down assay using a biotinylated DNA probe corresponding to the -116/+107 region of the wild-type (WT) or a mutant sequence of the A3B promoter in HepG2 cells stimulated with RelB plasmid for 24 hours. (F) Luciferase reporter assays in HEK293T cells transfected with the indicated plasmids for 24 hours. Dual-luciferase activity was determined. (G) RT-qPCR of A3B mRNA levels in HCCLM3 and PLC/PRF/5 cells exposed to LT $\alpha_1\beta_2$  for 24 hours. (H) Correlations among NFKB2, RELB and A3B in TCGA HCC tumour were denoted with Pearson's correlation coefficients. Error bars represent mean $\pm$ SEM. \* $P$ <0.05, \*\* $P$ <0.01, \*\*\* $P$ <0.001 (Student's t-test). A3B, APOBEC3B; LPS, lipopolysaccharide.

supplementary figure 4A). In addition, primary MDSCs with the conditioned medium from Hepa1-6-A3B cells displayed upregulated expression of immunosuppressive molecules, including ARG1, iNOS1 and PDL1 (online supplementary figure 4B). We separated the MDSCs from tumours and analysed immunosuppressive relevant genes expression. The immunosuppressive molecules, including ARG1, iNOS1, PDL1, CLEC7A and S100A9, displayed upregulated expression in MDSCs isolated from Hepa1-6-A3B tumours (online supplementary figure 4C). We further investigated whether overexpression of A3B and TAMs or MDSCs markers were associated with prognosis of HCC in TCGA. Kaplan-Meier analysis revealed that HCC patients with high CD11b/CD68/A3B and CD11b/CD33/A3B expression significantly correlated with poor overall prognosis (figure 3M). Taken together, these data suggested that

hepatoma-intrinsic A3B acted as an immunomodulatory factor to promote HCC progression.

Furthermore, we established a sleeping beauty transposon-based mouse liver cancer model (SBTmLC), in which intrahepatic delivery of oncogene generates HCC.<sup>16</sup> The mA3 gene was stably delivered into hepatocytes via hydrodynamic tail- vein injection (HDI) of the sleeping beauty transposon vectors into C57BL/6J mice combined with a single intraperitoneal injection of the carcinogen DEN on day 14 (online supplementary figure 5A). We observed high tumour burden and rapid outgrowth of HCC in mice with intrahepatic delivery of mA3 (online supplementary figure 5B-D). Flow cytometry analysis demonstrated a significant increase of MDSCs (online supplementary figure 5E), TAMs (online supplementary figure 5F,G) and CD8 $^+$ PD1 $^+$  T cells (online supplementary figure 5H) in

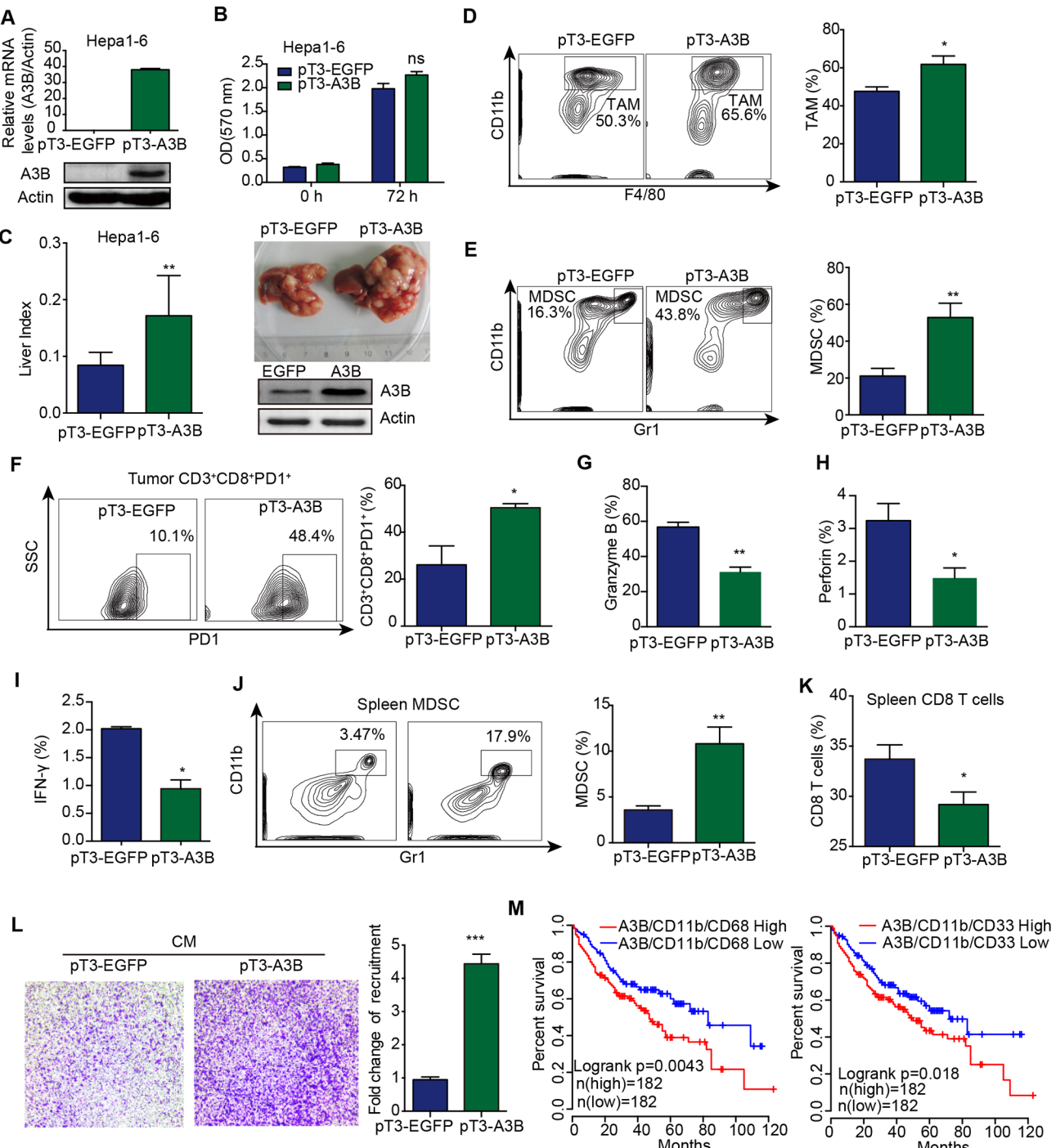


**Figure 3** A3B promotes HCC progression in immunocompetent mice associated with TAMs and MDSCs accumulation. (A) RT-qPCR and immunoblot assay of A3B mRNA and protein levels in Hepa1-6 cells with stably overexpressed A3B. (B) Proliferation assays of Hepa1-6-EGFP or Hepa1-6-A3B cells cultured under 10% FBS complete medium for 3 days. (C) Liver index and representative image of the Hepa1-6 orthotopic HCC tumours at 30 days after implantation. (D and E) The fractions of CD11b<sup>+</sup>Gr1<sup>+</sup>F4/80<sup>+</sup> TAMs (D) and CD11b<sup>+</sup>F4/80<sup>-</sup>Gr1<sup>+</sup> MDSCs (E) were determined by flow cytometry in tumours (n=6 mice per group). (F) The fraction of CD3<sup>+</sup>CD8<sup>+</sup>PD1<sup>+</sup> T cells was determined by flow cytometry in tumours (n=6 mice per group). (G–I) The fraction of CD8<sup>+</sup>PD1<sup>+</sup> T cells expressing granzyme (G), perforin (H) and IFN- $\gamma$  (I) were determined by flow cytometry in tumours (n=6 mice per group). (J and K) The fraction of MDSCs (J) and CD3<sup>+</sup>CD8<sup>+</sup> T cells (K) were determined by flow cytometry in mouse spleen with transplantation tumours (n=6 mice per group). (L) Transwell migration assay of immortalised bone marrow-derived macrophages (iBMDMs) attracted by 30% conditioned medium (CM) from Hepa1-6-EGFP and Hepa1-6-A3B cells. (M) Kaplan-Meier survival analysis for patients with HCC by log-rank test. Error bars represent mean $\pm$ SEM. \*p<0.05, \*\*p<0.01, \*\*\*p<0.001 (Student's t-test). A3B, APOBEC3B; CM, conditioned medium; HCC, hepatocellular carcinoma; MDSCs, myeloid-derived suppressor cells; OD, optical density; SSC, side scatter; TAMs, tumour-associated macrophages.

mA3 overexpressing mice compared with control mice. In order to further confirm the chemotaxis induced by mA3, we delivered mA3 into hepatocytes via HDI of the sleeping beauty transposon

vectors. Thirty days later, C57BL/6J mice were acutely challenged with DEN, followed by monocytes transplantation after 18 hours (online supplementary figure 5I). CD11b<sup>+</sup> monocytes

were labelled ex vivo with DiR tracker before transferring into the circulation of DEN-injected mA3 overexpressing mice. Mice were then imaged 12 hours post-transfusion by an *in vivo* imaging system for hepatic accumulation of labelled CD11b<sup>+</sup> monocytes, which were discovered to be more abundant in mA3 overexpressing mice (online supplementary figure 5J).

We next performed RNA-seq analysis to obtain global transcriptomic profiles in peritumour and tumour tissue in the SBTmLC model. RNA sequencing revealed a small fraction of genes differentially expressed on mA3 expression (online supplementary figure 6A and online supplementary figure 6D). Gene ontology (GO) analysis revealed that immune system pathway was one of the most significantly upregulated pathway in peritumour and tumour tissues with mA3 overexpression (online supplementary figure 6B and online supplementary figure 6E). Cell type analysis revealed that monocyte-macrophage cells were evidently enriched in peritumour and tumour tissues of mA3 overexpression (online supplementary figure 6C and online supplementary figure 6F). Besides, gene set enrichment analysis (GSEA), using well-established immune expression signatures<sup>17</sup> and the 39 MDSC genes,<sup>18</sup> corroborated these immune landscapes (online supplementary figure 6G-I). These data support that hepatocellular mA3 activates HCC initiation.

### Hepatoma-intrinsic A3B promotes the expression of CCL2, IL-34 and BMP7 to accumulate MDSCs and TAMs

To investigate the factor responsible for accumulated intratumoral TAMs and MDSCs, we performed a RNA-sequence analysis of Hepa1-6-A3B versus Hepa1-6-EGFP cells. GO analysis revealed that the immune response genes were the most prominent group (figure 4A). Secreted factors including CCL2, CCL5, IL-8, BMP7 and IL-34 were upregulated in Hepa1-6-A3B cells (figure 4A). Subsequently, we verified the RNA-sequence data by RT-qPCR (online supplementary figure 7A). We next performed a comparative analysis of RNA-sequence data between Hepa1-6-A3B cells and the SBTmLC model. Here, we focused on CCL2, IL-34 and BMP7 because they play an important role in cancer progression and found they were upregulated in both Hepa1-6-A3B cells and SBTmLC model (online supplementary figure 7A,B). Subsequently, we examined the expression of CCL2, IL-34 and BMP7 in HCC cell lines. Hepa1-6-A3B cells exhibited a higher expression of CCL2, IL-34 and BMP7 compared with Hepa1-6-EGFP cells (figure 4B). Ectopic A3B also increased the secretion of CCL2, IL-34 and BMP7 (figure 4C). Accordingly, CCL2, IL-34 and BMP7 expression in MHCC97H, MHCC97L, HCCLM3 and PLC/PRF/5 cell lines were lower in siA3B-treated cells than in control cells (figure 4D). Since tumour necrosis factor alpha(TNF- $\alpha$ ) and lymphotoxin(LT $\alpha_1\beta_2$ )play an important role in HCC progression,<sup>13 19</sup> we further examined whether the expression of CCL2 and IL-34 was A3B dependent. Knocking down endogenous A3B in MHCC97H cells reduced the expression of CCL2 and IL-34 induced by TNF- $\alpha$  or LT $\alpha_1\beta_2$  (online supplementary figure 7C). Similarly, moderate correlation between A3B and CCL2 was detected in human HCC (figure 4E). The A3B expression also slightly correlated with IL-34 and BMP7. These results suggested that CCL2, IL-34, and BMP7 are target genes that are activated by endogenous A3B in HCC cells.

We next examined whether A3B-induced CCL2 secretion is critical for the migration of macrophages. The conditioned medium from Hepa1-6-A3B cells increased the migration of iBMDM cells, whereas treatment with a CCR2 antagonist

(MK0812) inhibited iBMDM chemotaxis induced by the conditioned medium (online supplementary figure 7D). Using a consistent experimental approach in online supplementary figure 5I, we used RT-qPCR and ELISA to analyse mRNA and protein levels of chemokine on total liver parenchymal cells. The results showed that CCL2 was upregulated by mA3 in primary hepatocytes, whereas there was no significant difference between the two groups in the expression of IL-34 and BMP7 (online supplementary figure 7E). Similarly, RS102895, a CCR2 antagonist, can limit the chemotactic effects of monocytes to the liver (online supplementary figure 7F). It has been reported that IL-34 can recruit TAMs and promote M2 macrophage polarisation.<sup>20</sup> BMP7 was one of the members in TGF superfamily and induced M2 polarisation.<sup>21</sup> In fact, the neutralisation of A3B-induced cytokines (IL-34 and BMP7) attenuated expression of the ARG1 gene in iBMDMs (online supplementary figure 7G,H) and bone marrow-derived macrophages (online supplementary figure 7I,J).

Moreover, *in vivo* treatment using the CCR2 antagonist inhibited tumour growth in Hepa1-6-A3B tumour-bearing C57BL/6J mice (figure 4G-4I and online supplementary figure 7K). To confirm the critical role of IL-34 and BMP7 in A3B-mediated tumour progression, we knocked down IL-34 and BMP7 in Hepa1-6-A3B cells (figure 4F). The knockdown of IL-34 and BMP7 in Hepa1-6-A3B reduced tumour progression (figure 4G-4I and online supplementary figure 7K). Flow cytometric analysis revealed that the percentages of TAMs (figure 4J), M-MDSCs (figure 4K) and CD3<sup>+</sup>CD8<sup>+</sup>PD1<sup>+</sup> T cells (figure 4L) were decreased in RS102895-treated Hepa1-6-A3B tumours, Hepa1-6-A3B-shIL34 and Hepa1-6-A3B-shBMP7 tumours. Taken together, these data suggested that hepatoma-intrinsic A3B potentially promotes HCC progression by mediating TAMs and MDSCs accumulation.

### A3B promotes HCC progression *in vivo* through deaminase-independent activity

A3B contains two zinc coordinating cytidine deaminase activity (CDA) domains at positions 68 and 255 in the N-terminal and C-terminal domains, respectively.<sup>22</sup> We constructed a A3B mutant plasmid containing the substitution of glutamic acid residues at positions 68 and 255 to glutamine, which inhibits the CDA. We next used a fluorescence-based DNA C-to-U assay to study A3B CDA in HCC cell lines. No deaminase activity was observed in nuclear extracts from A3B or A3B<sup>E68Q/E255Q</sup> overexpression HepG2 cells (online supplementary figure 8A). Similar results were obtained with an endogenous A3B knockdown construct in the MHCC97L cell line (online supplementary figure 8B). A3B induction did not increase  $\gamma$ -H2AX focus formation (online supplementary figure 8C). We analyzed mutagenesis in primary tumours by APOBEC cytidine deaminases from TCGA integrated data in the FireBrowse database. In contrast to BRCA, we saw no enrichment of the APOBEC mutation pattern in HCC samples, similar to previous reports (online supplementary figure 8D). To further confirm the role of CDA domains of A3B in the HCC progression, A3B<sup>E68Q/E255Q</sup> overexpression Hepa1-6 cell line was generated by the sleeping beauty transposon system (figure 5A). The expression of A3B<sup>E68Q/E255Q</sup> in Hepa1-6 mouse cell line similarly failed to induce proliferation *in vitro* (figure 5B). Ectopic A3B and A3B<sup>E68Q/E255Q</sup> increased the secretion of CCL2, IL-34 and BMP7 (figure 5C). We next examined the effect *in vivo* by implanting Hepa1-6-A3B and Hepa1-6-A3B<sup>E68Q/E255Q</sup> cells in C57BL/6J mice. The expression of A3B and A3B<sup>E68Q/E255Q</sup> in

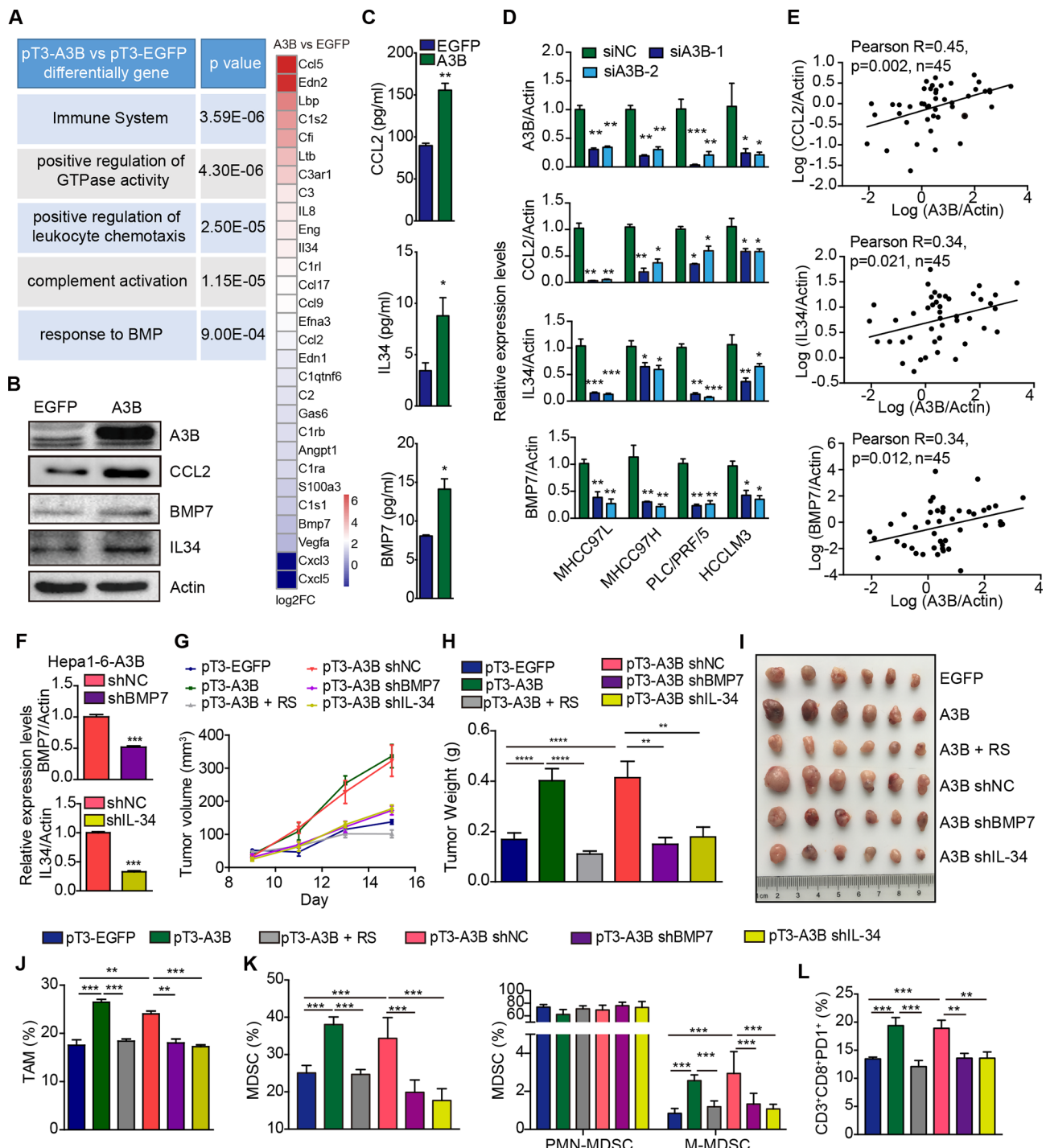


**Figure 4** A3B mediates TAMs and MDSCs accumulation induced by CCL2, IL-34 and BMP7 to promote HCC progression. (A) A table summarising the results of the RNA-seq data analysed by gene ontology; a heatmap showing the differentially expressed genes related to immune responses. (B) Immunoblot assays of CCL2, IL-34 and BMP7 protein levels in Hepa1-6-A3B cells. (C) ELISA for analysing the level of secreted CCL2, IL-34 and BMP7 in Hepa1-6-EGFP and Hepa1-6-A3B cells. (D) RT-qPCR analysis of A3B, CCL2, IL-34 and BMP7 mRNA in MHCC97H, MHCC97L, PLC/PRF/5 and HCCLM3 cells with A3B knockdown. (E) The mRNA level of A3B, CCL2, IL-34 and BMP7 relative to ACTIN was measured by RT-qPCR. Correlations among CCL2, IL-34, BMP7 and A3B in HCC tumour were denoted with Pearson's correlation coefficients. (F) RT-qPCR assay of IL-34 and BMP7 mRNA in Hepa1-6-A3B cells with lentivirus of shIL34 and shBMP7. (G and H) Graph showing tumour volume (G) and tumour weight (H) of Hepa1-6-A3B subcutaneous HCC tumours. Mice were treated twice a day by intraperitoneal (i.p.) injection with vehicle or RS102895 (5 mg/kg) (n=6 mice per group). (I) Photos of Hepa1-6-formed tumours. (J–L) The fractions of TAMs (J), MDSCs (K) and CD3<sup>+</sup>CD8<sup>+</sup>PD1<sup>+</sup> T cells (L) were determined by flow cytometry in Hepa1-6-A3B subcutaneous HCC tumours as indicated in figure 4I (n=6 mice per group). Error bars represent mean±SEM. \*p<0.05, \*\*p<0.01, \*\*\*p<0.001 (Student's t-test and one-way ANOVA). ANOVA, analysis of variance; A3B, APOBEC3B; HCC, hepatocellular carcinoma; IL, interleukin; TAMs, tumour-associated macrophages.

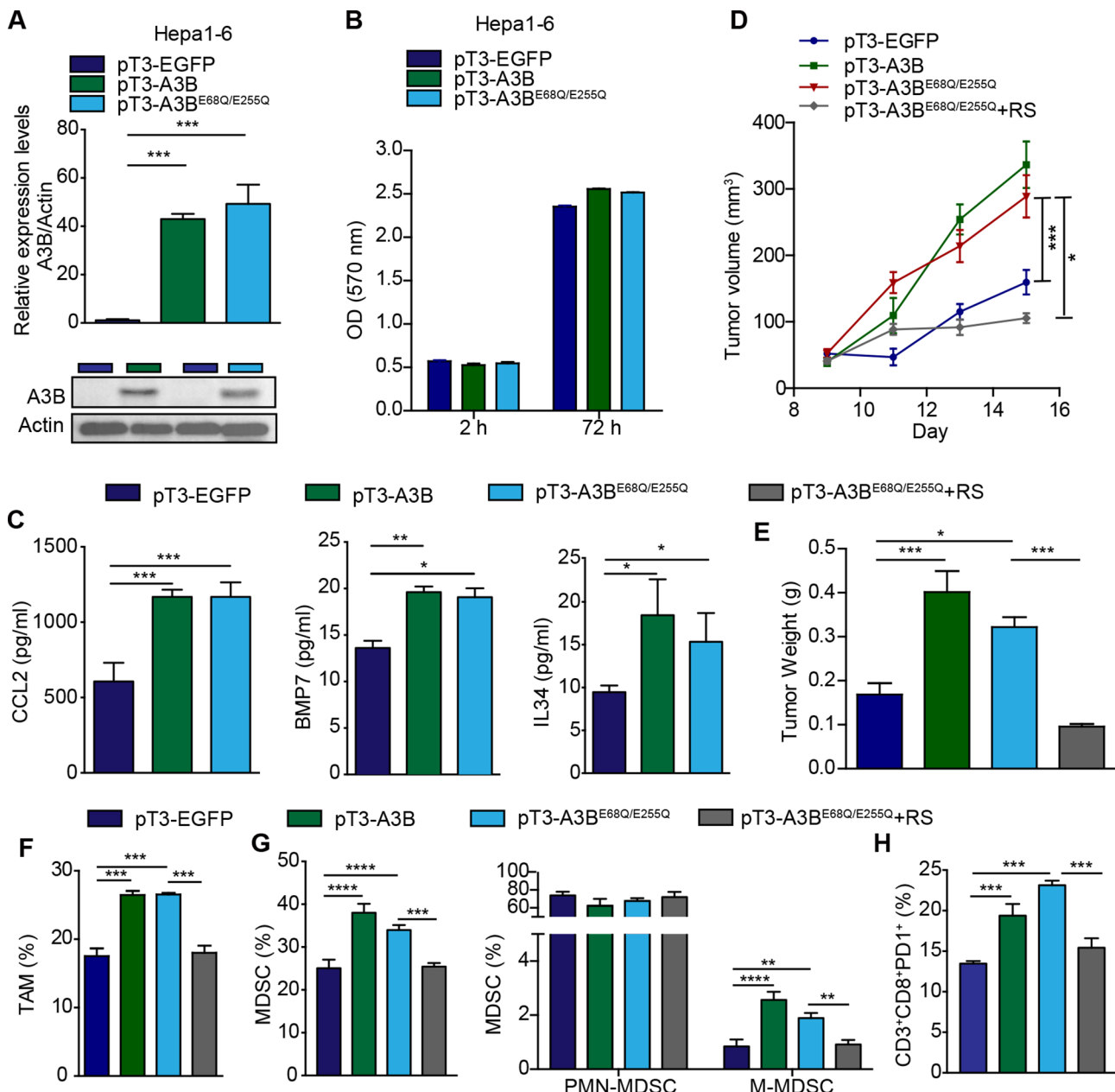


**Figure 5** A3B promotes HCC progression in vivo through deaminase-independent activity. (A) RT-qPCR and immunoblot assay of A3B mRNA and protein levels in Hepa1-6 cells with stably overexpressed A3B and A3B<sup>E68Q/E255Q</sup>. (B) Proliferation assays of Hepa1-6-EGFP or Hepa1-6-A3B cells cultured under 10% FBS complete medium for 3 days. (C) ELISA for analysing the level of secreted CCL2, IL-34 and BMP7 in A3B and A3B<sup>E68Q/E255Q</sup> overexpression Hepa1-6 cells. (D and E) Graph showing tumour size (D) and weight (E) of Hepa1-6-A3B subcutaneous HCC tumours after 15 days after implantation. Mice were treated twice a day by i.p. injection with vehicle or RS102895 (5 mg/kg) (n=6 mice per group). (F–H) The fractions of TAMs (F), MDSCs (G) and CD3<sup>+</sup>CD8<sup>+</sup>PD1<sup>+</sup> T cells (H) were determined by flow cytometry in Hepa1-6-A3B subcutaneous HCC tumours as indicated in figure 5E (n=6 mice per group). Error bars represent mean±SEM. \*p<0.05, \*\*p<0.01, \*\*\*p<0.001 (Student's t-test and one-way ANOVA). ANOVA, analysis of variance; HCC, hepatocellular carcinoma; IL, interleukin; MDSC, myeloid-derived suppressor cells; TAM, tumour-associated macrophage.

Hepa1-6 cells increased the tumour size/weight compared with the Hepa1-6-EGFP (figure 5D,E). Moreover, in vivo treatment using the CCR2 antagonist inhibited tumour growth in Hepa1-6-A3B<sup>E68Q/E255Q</sup> tumour-bearing C57BL/6J mice (figure 5D,E). The Hepa1-6-A3B<sup>E68Q/E255Q</sup>-formed tumours had an increased infiltration of TAMs and MDSCs and CD3<sup>+</sup>CD8<sup>+</sup>PD1<sup>+</sup> cells. In vivo treatment using the CCR2 antagonist inhibited infiltration of TAMs (figure 5F), M-MDSCs (figure 5G) and CD3<sup>+</sup>CD8<sup>+</sup>PD1<sup>+</sup> T cells (figure 5H). Taken together, these data suggested that A3B promotes HCC progression through deaminase-independent activity.

#### A3B induces expression of CCL2, IL-34 and BMP7 by modulating the repressive H3K27me3 marks

To investigate the mechanism of A3B-induced target gene transcription, we performed GSEA analysis and found significant overlaps in the H3K27me3-targeted genes between our RNA sequencing and published microarray data sets (figure 6A). It has been reported that DZNep, an inhibitor of H3K27me3 synthesis, could increase CCL2, IL-8, C3 and CCL5 in breast cancer.<sup>23</sup> These results suggested that the epigenetic H3K27me3 modification probably mediates A3B-induced transcriptional

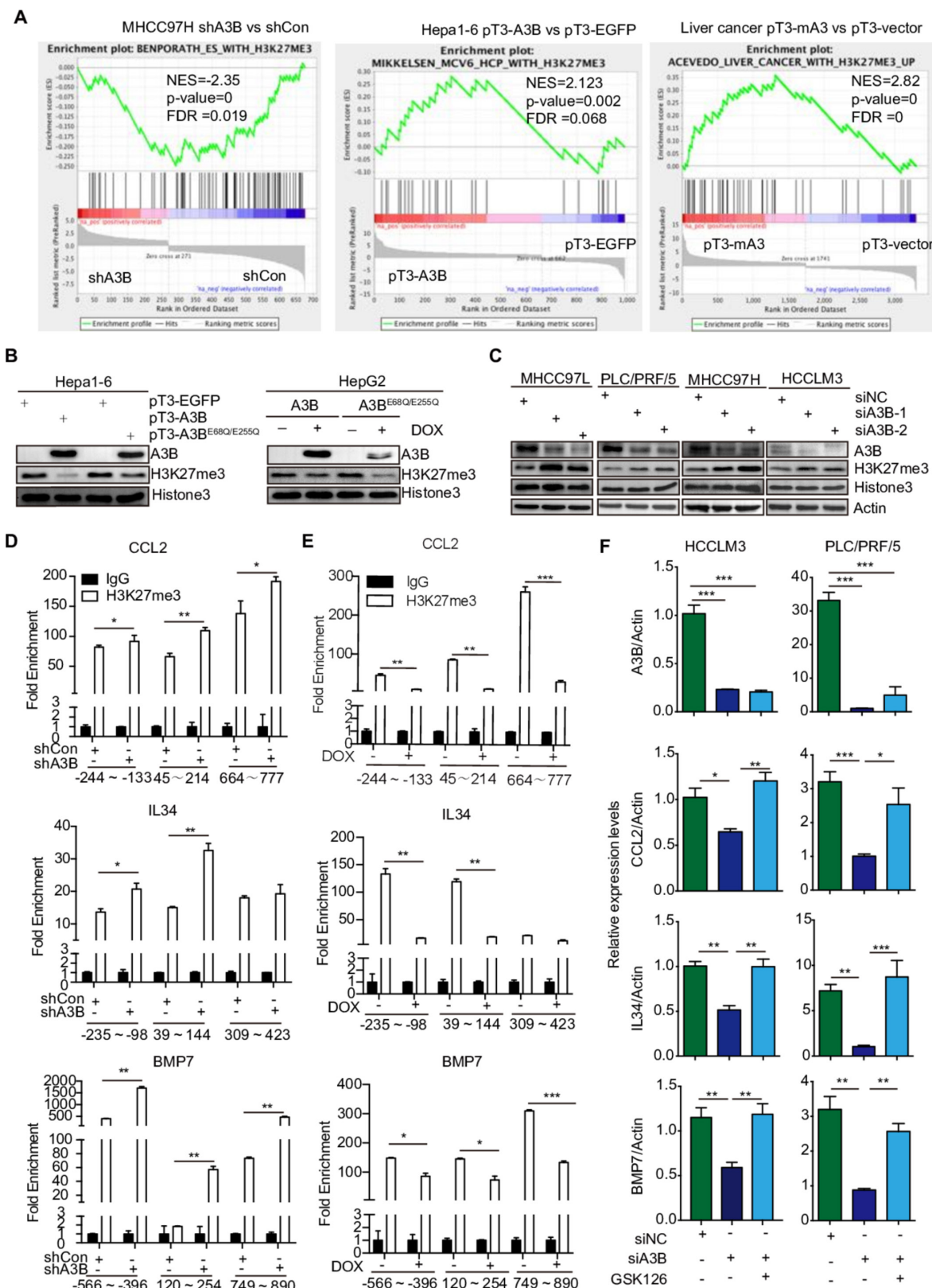


**Figure 6** A3B induces expression of CCL2, IL-34 and BMP7 by modulating the repressive mark H3K27me3. (A) GSEA analysis of the RNA-seq data in MHCC97H-shA3B versus MHCC97H- shCon, Hepa1-6-A3B versus Hepa1-6-EGFP, and SBTmLC model. (B) Immunoblot assays of indicated proteins in HepG2-Teton-A3B cells exposed to doxycycline (2 µg/mL) for 24 hours and Hepa1-6 cells. (C) Immunoblot assays of indicated proteins in MHCC97H, MHCC97L, PLC/PRF/5 and HCCLM3 cells with A3B knockdown. (D–E) ChIP-qPCR assays in HCCLM3 cells (D) with A3B knockdown, and in HepG2-Teton-A3B cells (E) exposed to doxycycline (2 µg/mL) for 24 hours. (F) RT-qPCR analysis of CCL2, IL-34 and BMP7 mRNA levels in PLC/PRF/5 and HCCLM3 cell with A3B knockdown exposed to GSK126 (1 µM) for 48 hours. Error bars represent mean±SEM. \* $p<0.05$ , \*\* $p<0.01$ , \*\*\* $p<0.001$  (Student's t-test and one-way ANOVA). A3B, APOBEC3B; ANOVA, analysis of variance; GSEA, gene set enrichment analysis; HCC, hepatocellular carcinoma; IL, interleukin.

activation. In accordance with these studies, our results showed that upregulation of A3B and A3B<sup>E68Q/E255Q</sup> expression reduced H3K27me3 levels in HepG2 and Hepa1-6 cells (figure 6B), while knockdown of A3B in PLC/PRF/5, MHCC97H, MHCC97L and HCCLM3 cells increased H3K27me3 abundance (figure 6C). We next performed ChIP assays to analyse H3K27me3 at the promoters of CCL2, IL-34 and BMP7. ChIP-qPCR assays showed that H3K27me3 was laid down at the promoters of CCL2, IL-34 and BMP7 by upregulation of A3B expression in HepG2 cells (figure 6E), whereas endogenous A3B knockdown in HCCLM3 cells increased H3K27me3 levels at the CCL2, IL-34 and BMP7 promoters (figure 6D). As anticipated, GSK126, an inhibitor of H3K27me3 synthesis, induced re-expression of CCL2, IL-34 and BMP7 in A3B knockdown cells of PLC/PRF/5 and HCCLM3 cells (figure 6F). Thus, A3B can repress epigenetic modulation of H3K27me3, implicated in transcription of several cytokines.

### A3B associates with the PRC2 complex in HCC cells

PRC2 is required to maintain methylation of H3K27 in multicellular organisms.<sup>24</sup> Chemokine expression is regulated by cancer-intrinsic genetic and epigenetic mechanisms such as the DNA methylation and PRC2.<sup>25</sup> PRC2 consists of three core protein subunits—SUZ12, EED and EZH2. We next investigated whether the negative correlation between H3K27me3 and A3B might have a biochemical basis associated with PRC2. To this end, His-tagged A3B was expressed in HepG2 cells and nuclear extracts immunoprecipitated with anti-His-tag magnetic beads and probed with EZH2, EED and SUZ12 antibodies. All three proteins were found in the immunoprecipitate indicating that A3B interacts with the intact PRC2 complex (figure 7A). Next, we showed that endogenous SUZ12, EED and EZH2 immunoprecipitated exogenous A3B from HepG2 cell nuclear extracts, indicating that A3B interacted with EZH2, EED and SUZ12 (figure 7A). The interaction between endogenous A3B and the PRC2 complex was also observed in HCCLM3 cells (figure 7B). To determine whether the A3B-PRC2 association is direct, baculovirus-produced and purified SUZ12, EZH2, EED and *Escherichia coli*-purified A3B tested positive in immunoprecipitation assays, indicating that A3B robustly interacts with PRC2 and that such interaction did not require additional proteins (figure 7C). An immunofluorescence assay also showed the colocation of between A3B and PRC2 (figure 7D). We next generated N-terminally and C-terminally truncated A3B mutants (NDT: 1-190aa and CDT: 191-382aa) and tested for their ability to interact with PRC2. Flag-tagged EZH2, SUZ12, EED and N-terminally and C-terminally truncated A3B mutants were coexpressed in different combinations in 293T cells and cell extracts immunoprecipitated. We found that the C-terminally truncated A3B mutants robustly interacts with PRC2 (figure 7E). To address whether A3B affects PRC2 target occupancy, we performed ChIP assays to analyse EZH2 at promoters of CCL2, IL-34 and BMP7. Over expression of A3B by Dox treatment resulted in downregulation of EZH2 occupancy at the promoters of CCL2, IL-34 and BMP7 (figure 7F), whereas endogenous A3B knockdown in HCCLM3 cells increased EZH2 levels at the CCL2, IL-34 and BMP7 promoters (figure 7G). A similar change of EZH2 occupancy and H3K27me3 were observed at MYT-1 locus, a known EZH2 target gene (figure 7H-7I). These results demonstrate that A3B impair the binding of PRC2 to its target genes. To test whether, in addition to targeting, A3B can also regulate PRC2 enzymatic activity, we performed histone methyltransferase (HMT) assays with purified recombinant PRC2 complex and A3B. Interestingly, A3B in vitro was sufficient to inhibit

PRC2 HMT activity in a dose-dependent manner (figure 7J). In support of the notion that A3B depresses global H3K27me3 abundance, negative correlation among A3B and H3K27me3 expressions were detected in human HCC (figure 7K). We found that lower H3K27me3 level in HCC cell lines (PLC/PRF/5, MHCC97H and HCCLM3) with higher A3B expression and higher H3K27me3 level in HCC cell lines (HepG2) with lower A3B expression (figure 7L). Taken together, our results demonstrate that A3B negatively regulates PRC2 function in HCC cells.

### DISCUSSION

The chronic inflammation microenvironment is one of the main features of HCC. In this study, we have shown that A3B is a novel direct non-canonical NF-κB target gene in HCC cells. In other studies, the 5'-GGRRNNYYCC-3' consensus κB site sequence was used to investigate the occupancy of NF-κB transcription factor on the A3B promoter. However, it has been reported that the RelB:p52 heterodimer binds to and activates a unique class of genes that contain κB sites that diverge significantly from classic κB sites.<sup>26</sup> The RelB:p52 complex seems to interact through the flanking GG:CC core elements with more contiguous and centrally located A:T base pairs.<sup>26</sup> Our results indicated that RelB directly binds to the GGGGAAAC sequence at the A3B gene promoter to activate its transcription. We found that A3B in tumour cells could enhance TAMs and MDSCs infiltration into tumours in C57BL/6J mice. This means that hepatoma-intrinsic A3B and immune cells form a positive feedback loop, resulting in a chronic inflammatory microenvironment in the liver.

Our results show that the chemokine CCL2 is upregulated in A3B overexpressing tumour cells, which contributes to the recruitment of TAMs and MDSCs. CCL2, highly expressed in microenvironment of many types of cancer including lung cancer, breast cancer and liver cancer, can recruit monocytes and macrophages into tumours to stimulate tumour cell survival and confer immune evasion. RNA sequencing also revealed a series of chemokines and cytokines, such as IL-34, CCL5, BMP7, VEGF, IL-8 and C3, were upregulated in A3B overexpressing tumour cells, all of which contributed to the accumulation of TAMs and MDSCs. Hence, A3B may be an upstream member in the transcriptional regulation of cytokines, and the intervention of A3B functions may exhibit more effective antitumour effects compared with the use of chemokine inhibitors alone.

PRC2 is involved in the establishment of a repressed chromatin state through H3K27me3 and regulates expression of some genes.<sup>27</sup> Our results demonstrate that A3B upregulation in HCC depressed global H3K27me3 abundance via interaction with PRC2, which is independent of cytosine deaminase pathways, and reduced the presence of H3K27me3 at promoters of CCL2, IL-34 and BMP7. It has been reported knockout of EZH2 in bone marrow cells did not have any influence on cell proliferation but increased inflammatory cytokines to damage normal bone marrow cells.<sup>28</sup> Additionally, EZH2 loss dramatically promotes Kras-driven lung adenocarcinoma formation and exacerbated the inflammatory response.<sup>29</sup> Therefore, the disturbing non-enzymatically dependent function of A3B may inhibit a variety of chemokine-mediated immunosuppressive microenvironments (figure 8).

It has been reported that A3B induced the conversion of cytosine to uracil in the minus-sense single-strand HBV DNA, leading to G-to-A hypermutations in the subsequent plus-strand viral DNA.<sup>30</sup> However, A3B is upregulated in patients with chronic HBV infection or HCC.<sup>6,7</sup> The hepatocarcinogenesis in patients with chronic HBV infection is a long-term pathological

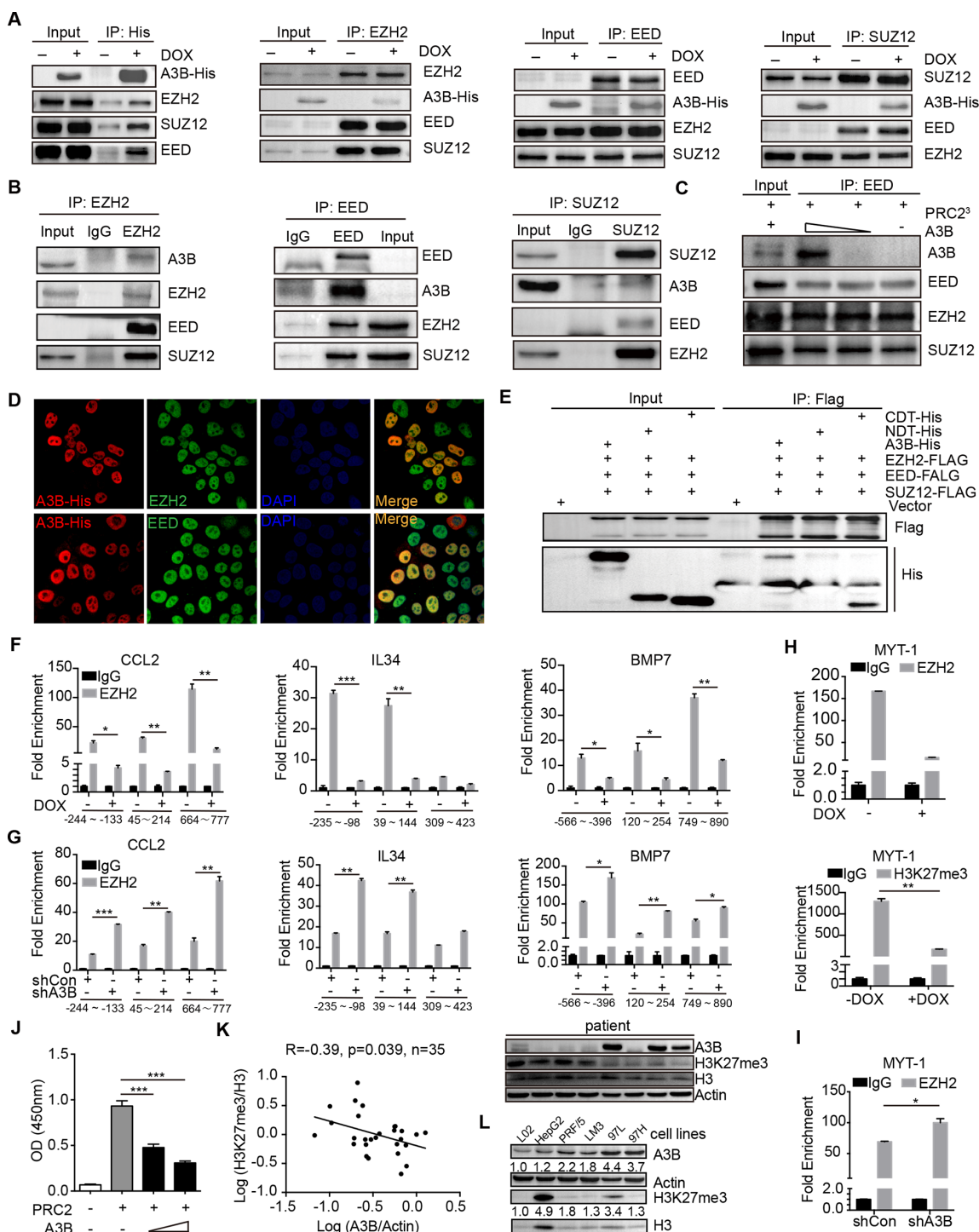


**Figure 7** A3B directly interacts with the PRC2 complex in HCC cells. (A) Coimmunoprecipitation assays of exogenous A3B and EZH2, EED or SUZ12 in HepG2-Teton-A3B cells exposed to doxycycline (2 µg/mL) for 24 hours. (B) Coimmunoprecipitation assays analysis of interaction between endogenous A3B and EZH2, EED or SUZ12 in HCCLM3 cells. (C) Baculovirus-expressed EZH2, SUZ12, EED-Flag proteins and *Escherichia coli*-purified A3B were incubated and immunoprecipitated with a Flag resin antibody. Immunocomplexes were subjected to immunoblotting with A3B, EZH2, EED or SUZ12 antibodies. (D) Immunofluorescence analysis of binding of A3B to EZH2 or EED in HepG2-Teton-A3B cells exposed to doxycycline (2 µg/mL) for 24 hours. (E) Extracts from 293T transfected cells were immunoprecipitated with Flagresin and immunoblotted with either His or Flag antibodies. (F and G) ChIP-qPCR assays in HepG2-Teton-A3B cells (F) exposed to doxycycline (2 µg/mL) for 24 hours and in HCCLM3 cells (G) with A3B knockdown. (H and I) ChIP-qPCR assays for MYT-1 locus in HepG2-Teton-A3B cells (H) exposed to doxycycline (2 µg/mL) for 24 hours and in HCCLM3 cells (I) with A3B knockdown. (J) Histone methyltransferase assays. (K) The protein level of A3B relative to ACTIN and H3K27me3 relative to H3 was measured by western blot. Correlations among A3B relative to ACTIN and H3K27me3 relative to H3 in HCC tumour were denoted with Pearson's correlation coefficients. (L) Western blot analysis of the A3B protein level relative to ACTIN and H3K27me3 protein level relative to H3. The numbers below the A3B blot stand for the ratio of A3B protein level to actin level in each cell line. The numbers below the H3K27me3 blot stand for the ratio of H3K27me3 protein level to H3 level in each cell line. Error bars represent mean±SEM. \*p<0.05, \*\*p<0.01, \*\*\*p<0.001 (Student's t-test). A3B, APOBEC3B; HCC, hepatocellular carcinoma; IL, interleukin.

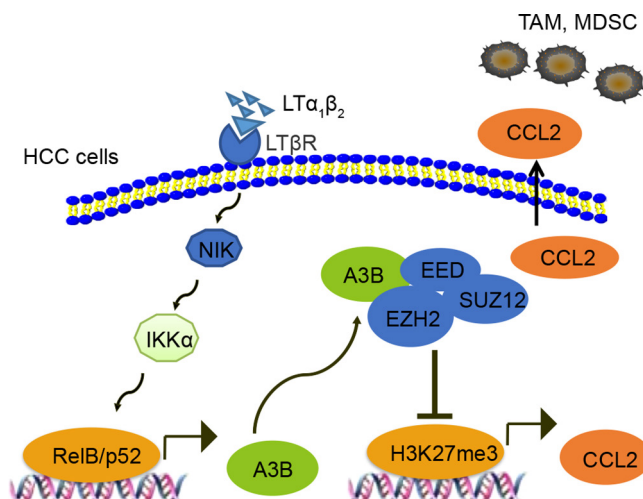


**Figure 8** Schematic depicting mechanisms of A3B-driven CCL2 expression and TAM and MDSC accumulation in HCC. A3B is upregulated through non-classical NF- $\kappa$ B pathway. A3B upregulation depresses global H3K27me3 abundance via interaction with PRC2. This procedure reduces an occupancy of H3K27me3 on promoters of the chemokine CCL2 to increase the levels of CCL2 mRNA and protein, which recruits massive TAMs and MDSCs into the tumours. A3B, APOBEC3B; HCC, hepatocellular carcinoma; MDSC, myeloid-derived suppressor cell; TAM, tumour-associated macrophage.

process involving changes in the inflammatory microenvironment, DNA instability caused by HBV integration and evolution of HBV mutants.<sup>11–31</sup> At present, A3B-induced cccDNA mutation experiments used an in vitro cell line infection model, which did not adequately mimic the possible carcinogenic effects of HBV mutants. In fact, different HBV mutants such as A1762T/G1764A are significantly associated with HCC risks and predict the occurrence and poor prognosis of HCC.<sup>32</sup> In addition, it has been reported that A3B promotes the progression of HCC by producing a truncated HBx mutant protein.<sup>7</sup> However, viral clearance during HBV infection, CD8 $^{+}$  T lymphocytes is an important antiviral mechanism. Although our study did not involve HBV infection, our results may also suggest that the A3B-mediated inflammatory microenvironment plays a vital role in the immune escape of HBV. Future study may further screen or develop novel compounds to interrupt the interaction of A3B and PRC2 complexes, which might be a new strategy for therapy and HCC immunotherapy.

**Correction notice** This article has been corrected since it published Online First. The significance of this study box has been updated.

**Acknowledgements** We kindly express our appreciation to Yumeng Shen (Public platform of State Key Laboratory of Natural Medicines) for her assistance of live cell sorting.

**Contributors** YY and DW conceived the project and designed the experiments. DW performed the study, analysed the data and wrote the paper. JN, YL, SZ, XC, JY, YZ, SR, RS and MY performed the study. DC and GW analysed the data. YY and XJ analysed the data and critically revised the manuscript. YY and DW are responsible for the overall content as guarantors. Obtained funding: YY.

**Funding** This work was supported by the National Natural Science Foundation of China (Nos 81673468, 91529304, 81473230, 81403020, 81273547, 81502407 and 81703562), the 111 Project (No 111-2-07), the Jiangsu Province Natural Science Foundation of China (Nos BK2014666 and BK20170732) and 'Double First-Class' University project (No CPU2018GF10 and CPU2018GY46).

**Competing interests** None declared.

**Patient consent for publication** Obtained.

**Ethics approval** The Affiliated Drum Tower Hospital.

**Provenance and peer review** Not commissioned; externally peer reviewed.

## REFERENCES

- 1 Salter JD, Bennett RP, Smith HC. The APOBEC protein family: united by structure, divergent in function. *Trends Biochem Sci* 2016;41:578–94.
- 2 Roberts SA, Lawrence MS, Klimczak LJ, et al. An APOBEC cytidine deaminase mutagenesis pattern is widespread in human cancers. *Nat Genet* 2013;45:970–6.
- 3 Burns MB, Temiz NA, Harris RS. Evidence for APOBEC3B mutagenesis in multiple human cancers. *Nat Genet* 2013;45:977–83.
- 4 Alexandrov LB, Nik-Zainal S, Wedge DC, et al. Signatures of mutational processes in human cancer. *Nature* 2013;500:415–21.
- 5 Henderson S, Chakravarthy A, Su X, et al. APOBEC-mediated cytosine deamination links PIK3CA helical domain mutations to human papillomavirus-driven tumor development. *Cell Rep* 2014;7:1833–41.
- 6 Vartanian JP, Henry M, Marchio A, et al. Massive APOBEC3 editing of hepatitis B viral DNA in cirrhosis. *PLoS Pathog* 2010;6:e1000928.
- 7 Xu R, Zhang X, Zhang W, et al. Association of human APOBEC3 cytidine deaminases with the generation of hepatitis virus B x antigen mutants and hepatocellular carcinoma. *Hepatology* 2007;46:1810–20.
- 8 Seplavarski VB, Soldatov RA, Popadin KY, et al. APOBEC-induced mutations in human cancers are strongly enriched on the lagging DNA strand during replication. *Genome Res* 2016;26:174–82.
- 9 Haradhvala NJ, Polak P, Stojanov P, et al. Mutational strand asymmetries in cancer genomes reveal mechanisms of DNA damage and repair. *Cell* 2016;164:538–49.
- 10 Lucifora J, Xia Y, Reisinger F, et al. Specific and nonhepatotoxic degradation of nuclear hepatitis B virus cccDNA. *Science* 2014;343:1221–8.
- 11 Arzumanyan A, Reis HM, Feitelson MA. Pathogenic mechanisms in HBV- and HCV-associated hepatocellular carcinoma. *Nat Rev Cancer* 2013;13:123–35.
- 12 Wan S, Kuo N, Kryczek I, et al. Myeloid cells in hepatocellular carcinoma. *Hepatology* 2015;62:1304–12.
- 13 Haybaeck J, Zeller N, Wolf MJ, et al. A lymphotoxin-driven pathway to hepatocellular carcinoma. *Cancer Cell* 2009;16:295–308.
- 14 Elsharkawy AM, Mann DA. Nuclear factor- $\kappa$ B and the hepatic inflammation-fibrosis-cancer axis. *Hepatology* 2007;46:590–7.
- 15 Mátés L, Chuah MK, Belay E, et al. Molecular evolution of a novel hyperactive Sleeping Beauty transposase enables robust stable gene transfer in vertebrates. *Nat Genet* 2009;41:753–61.
- 16 Chen X, Calvisi DF. Hydrodynamic transfection for generation of novel mouse models for liver cancer research. *Am J Pathol* 2014;184:912–23.
- 17 Jojic V, Shay T, Sylvia K, et al. Identification of transcriptional regulators in the mouse immune system. *Nat Immunol* 2013;14:633–43.
- 18 Wang G, Lu X, Dey P, et al. Targeting YAP-Dependent MDSC infiltration impairs tumor progression. *Cancer Discov* 2016;6:80–95.
- 19 Nakagawa H, Umemura A, Taniguchi K, et al. ER stress cooperates with hypernutrition to trigger TNF-dependent spontaneous HCC development. *Cancer Cell* 2014;26:331–43.
- 20 Pyontek SM, Akkari L, Schuhmacher AJ, et al. CSF-1R inhibition alters macrophage polarization and blocks glioma progression. *Nat Med* 2013;19:1264–72.
- 21 Rocher C, Singla R, Singal PK, et al. Bone morphogenetic protein 7 polarizes THP-1 cells into M2 macrophages. *Can J Physiol Pharmacol* 2012;90:947–51.
- 22 Caval B, Bouzidi MS, Suspène R, et al. Molecular basis of the attenuated phenotype of human APOBEC3B DNA mutator enzyme. *Nucleic Acids Res* 2015;43:9340–9.
- 23 Sun F, Chan E, Wu Z, et al. Combinatorial pharmacologic approaches target EZH2-mediated gene repression in breast cancer cells. *Mol Cancer Ther* 2009;8:3191–202.
- 24 Cao R, Zhang Y, SUZ12 is required for both the histone methyltransferase activity and the silencing function of the EED-EZH2 complex. *Mol Cell* 2004;15:57–67.
- 25 Nagarsheth N, Wicha MS, Zou W. Chemokines in the cancer microenvironment and their relevance in cancer immunotherapy. *Nat Rev Immunol* 2017;17:559–72.
- 26 Fusco AJ, Huang DB, Miller D, et al. NF- $\kappa$ B p52:RelB heterodimer recognizes two classes of kappaB sites with two distinct modes. *EMBO Rep* 2009;10:152–9.
- 27 Sparmann A, van Lohuizen M. Polycomb silencers control cell fate, development and cancer. *Nat Rev Cancer* 2006;6:846–56.
- 28 Sashida G, Harada H, Matsui H, et al. Ezh2 loss promotes development of myelodysplastic syndrome but attenuates its predisposition to leukaemic transformation. *Nat Commun* 2014;5:4177.
- 29 Wang Y, Hou N, Cheng X, et al. Ezh2 acts as a tumor suppressor in kras-driven lung adenocarcinoma. *Int J Biol Sci* 2017;13:652–9.
- 30 Suspène R, Guérard D, Henry M, et al. Extensive editing of both hepatitis B virus DNA strands by APOBEC3 cytidine deaminases in vitro and in vivo. *Proc Natl Acad Sci U S A* 2005;102:8321–6.
- 31 Deng Y, Du Y, Zhang Q, et al. Human cytidine deaminases facilitate hepatitis B virus evolution and link inflammation and hepatocellular carcinoma. *Cancer Lett* 2014;343:161–71.
- 32 Yeh CT, So M, Ng J, et al. Hepatitis B virus-DNA level and basal core promoter A1762T/G1764A mutation in liver tissue independently predict postoperative survival in hepatocellular carcinoma. *Hepatology* 2010;52:1922–33.